

The biological membrane viewed as a heterogenous chemical system

As membranas biológicas analisadas como um sistema químico heterogéneo

WINCHIL L. C. VAZ¹ AND EURICO MELO²

¹ UNIVERSIDADE DO ALGARVE, 8000 FARO, PORTUGAL, AND

² INSTITUTO DE TECNOLOGIA QUÍMICA E BIOLÓGICA AND INSTITUTO SUPERIOR TÉCNICO, APARTADO 127, P-2780 OEIRAS, PORTUGAL

The biological membrane, a cellular structure that separates the cell from its environment and intracellular compartments from each other, is composed principally of a so-called "lipid bilayer" that is made up of two apposed monomolecular layers of amphiphilic lipids, generally phospholipids but also glycolipids and cholesterol. The lipid bilayer, a thin quasi-two-dimensional fluid film with two polar surfaces and an apolar core and a thickness of approximately 10 nm, acts as a solvent system for several proteins which may be dissolved in it or adsorbed to its surface. The chemical composition of the lipid bilayer is known to be complex, generally containing three or four lipid classes known to be not ideally miscible among themselves. This creates the conditions for a probable heterogeneity of the system in the physical-chemical sense. In fact, it is known that the two monomolecular layers of the lipid bilayer in many biological membranes have different chemical compositions, what corresponds to a transmembrane heterogeneity of the system. Microscopic (molecular scale) and macroscopic (cellular scale) in-plane heterogeneities are known to exist. Although to a chemist it is quite clear that between these two extremes (microscopic and macroscopic scales) a mesoscopic heterogeneity must also exist, this has not been clearly shown, to be the case for biological membranes primarily because of the non-existence of suitable techniques with the necessary spatial resolution for this sort of system. It must be emphasized, however, that the existence of mesoscopic heterogeneities in artificial lipid bilayers is today a generally accepted phenomenon.

Mesoscopic heterogeneity raises interesting questions with regard to phase topology which in its turn has important consequences for component distribution, percolation and chemical kinetics in the system. Here we shall address ourselves primarily to the questions of percolation and chemical kinetics emphasizing experimental and Monte Carlo simulations on model systems and the extrapolation of these results and their consequences for biological membranes.

A membrana biológica, a estrutura celular que separa a célula do seu ambiente exterior e também os compartimentos intracelulares uns dos outros, é composta essencialmente por aquilo a que se convencionou chamar "bicamada lipídica" que é constituída por duas monocamadas moleculares adjacentes formadas por lípidos anfifílicos, geralmente fosfolípidos, mas também glicolípidos e colesterol. A bicamada lipídica, um filme fluido quase-bidimensional de superfícies polares e centro apolar, com uma espessura de cerca de 10 nm, faz o papel de solvente para muitas proteínas que nela se incorporam ou se adsorvem à superfície. Esta bicamada lipídica natural tem uma composição química complexa, geralmente contendo três ou quatro classes de lípidos que se sabe não formarem misturas ideais. É, portanto, de prever que estas misturas apresentem heterogeneidade química-física. De facto, em muitas membranas biológicas as duas monocamadas constituintes da bicamada lipídica têm composição diferente, donde resulta uma heterogeneidade transmembranar. Porém, também se sabe existem heterogeneidades, quer microscópicas (à escala molecular) quer macroscópicas (à escala celular) no plano da membrana. De um ponto de vista estritamente químico não pode deixar de existir também, entre estes dois extremos (heterogeneidade microscópica e macroscópica), uma heterogeneidade mesoscópica, embora esta nunca tenha sido evidenciada de uma forma indubitável no caso de membranas biológicas. Não podemos esquecer que não existem, actualmente, técnicas com a resolução espacial necessária para a observação destes sistemas sem criar perturbações que ponham em dúvida os resultados. Em bicamadas lipídicas artificiais a existência de heterogeneidade mesoscópica está actualmente experimentalmente provada. Reconhecida a existência de heterogeneidade mesoscópica, fica em aberto a sua topologia que, por sua vez, condiciona a distribuição de solutos e componentes, e, em consequência, a difusão/percolação e cinética das reacções químicas no sistema. No presente trabalho abordamos os problemas levantados pela percolação e compartimentalização de reagentes em sistemas modelo, analisados quer experimentalmente quer por simulação e discutimos as consequências da extrapolação dos resultados obtidos ao caso de membranas biológicas.

Introduction

Our current understanding of the biological membrane has its origin in a report by Gorter and Grendel [1], that was subsequently developed by reports from various researchers of which the landmark papers of Danielli and Davson [2], Robertson [3] and Singer and Nicolson [4] merit special mention. Today, the generally accepted working hypothesis is that the biological membrane is a "fluid mosaic" composed basically of a mostly, if not completely, fluid lipid bimolecular layer as its basal structure with proteins "extrinsically" adsorbed to the polar surfaces of the layer or "intrinsically" dissolved in the fluid sheet. The crucial point that is made in this model is that the membrane is a quasi-two dimensional fluid sheet and all its components (lipids and proteins) are, in principle, free to diffuse (rotationally and translationally) in the plane of the sheet. A homogeneous state, in the physical-chemical sense, is generally assumed for the lipid bimolecular fluid layer. While this model has helped advance our understanding of the structure and dynamics of biological membranes and their physiological role in the cell, in that it has stimulated a considerable amount of research in the area, it leaves many questions of a more quantitative nature unanswered.

Very early studies [5] showed that under certain conditions lipids in bilayers showed immiscibility both in the solid and fluid phases. These studies have been since confirmed and extended by several workers (for a collection of data see [6]) and, from the several phase diagrams for lipid bilayers formed from binary lipid mixtures that are available now, the conclusion can be drawn that lipid immiscibility in bilayers is more the rule than the exception. This would lead us to expect that the biological membrane or, more particularly, its lipid bilayer is more probably a heterogenous system rather than a homogenous one. This has, in fact, been observed to be the case at several levels. Macroscopic heterogeneities (over dimensions that are more comparable with those of the cell than of the molecular constituents) in biological membranes have now been quite well established. Careful analysis of the chemical composition of the inner and outer leaflets of several cellular membranes shows that the two halves of these membranes have distinct compositions. Besides this inside-outside heterogeneity, a clearly defined macroscopic lateral heterogeneity, often termed "functional polarity", has been clearly shown in some cell types, epithelial cells [7] and hepatocytes [8] being some of the best studied cases from this point of view. Another form of membrane heterogeneity is observed at the microscopic level (comparable to molecular dimensions) and arises from the specific interaction of membrane components among themselves as is the case in the so-called "boundary lipid" layer around integral membrane proteins.

If immiscibility is assumed, the two-dimensional nature of the membrane should also permit heterogeneity at a mesoscopic (several 10^2 to 10^4 times molecular dimensions) level [9, 10]. Such a mesoscopic heterogeneity, while being extremely difficult to clearly demonstrate due to unavailability of experimental methods with an adequate resolution, would explain a large number of observations with regard to the dynamics of membrane constituents [9]. Jain [11] has proposed that the lipid bilayer in the fluid mosaic model should include a phase heterogeneity that results in an overall non-random distribution of components in the system. We have subscribed this point of view [12, 13] and discussed some of the consequences of this refinement of the fluid mosaic model [9, 14].

In the present paper we propose to briefly review some concepts on biological membrane heterogeneity, discuss its causes and consequences and attempt to propose new lines of research that may be important for our understanding of the complex functions of this important cellular structure.

Phase Behaviour in Lipid Bilayers

Artificial lipid bilayers, which form spontaneously when certain phospholipids are hydrated, have provided many important insights into the structural and dynamic properties of the biological membrane. While the results of studies on these systems are not always directly translatable to the lipid bilayer in a biological membrane, they do provide excellent points of reference for the understanding of these. Model lipid bilayers prepared from most of the classes of lipids commonly encountered in biological membranes are lyotropic, thermotropic and barotropic smectic liquid crystal systems that undergo specific phase transitions between one or several ordered phases and disordered phases [15]. The ordered phases typically occur at low (<40 weight %) water content, low temperatures and/or very high pressures, all of which are not very significant from the biological point of view. They are characterized by a high degree of conformational order in the lipid acyl chains and positional order of the lipid chains and of the lipids themselves over long ranges in the plane of the bilayer. The disordered (often called fluid, liquid or liquid crystalline) phases are of more biological relevance in that these are the phases found in most biological membranes under normal conditions. These phases are characterized by low conformational order in the chains and lack of long range positional order in the plane of the bilayer. A characteristic example of lipid bilayer polymorphism in a single-component lipid bilayer under constant pressure and in excess water is shown in Figure 1 in which the transitions between different phases is thermally triggered. The temperatures at which these transitions occur are dependent on the nature of the phospholipid "head groups" (polar parts that are expo-

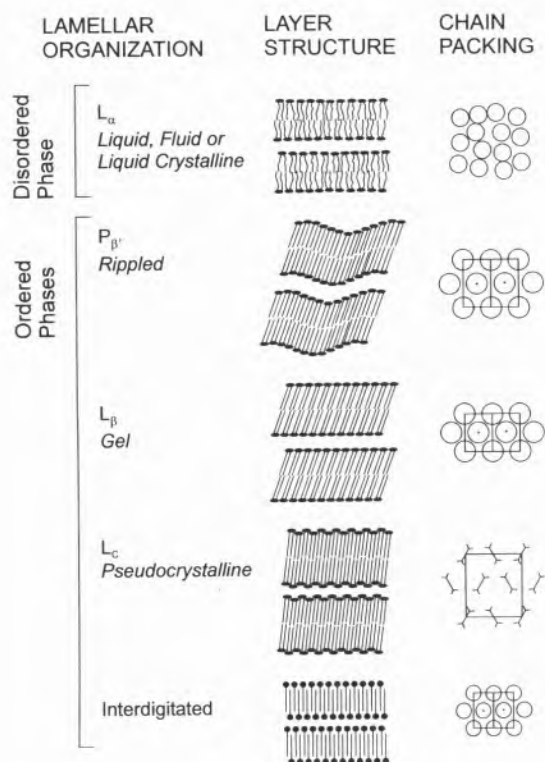


Figure 1 – Diagrams showing the layer structures and chain packing arrangements for the thermotropic phases found for pure phospholipids at constant pressure in excess water.

sed to water in the bilayer) as well as the lengths and degree and position of unsaturation of the acyl chains. When ionizable lipids are involved, the local pH and ionic strength of the aqueous phase in contact with the bilayer must also be specified since these also influence the bilayer polymorphism [16]. It is important to bear the complexity of this polymorphism in mind when considering bilayers that are composed of several constituent lipids as is the case in biological membranes.

We shall not address ourselves here to a consideration of the complexity of phase behaviour in the biological membrane. The problem is probably not addressable with the level of information we are presently capable of obtaining and processing. Rather, it is our intention to exemplify the consequences of phase separations in the lipid bilayers, as models for the far more complicated biological membranes, using simple two-phase bilayers prepared from binary lipid mixtures in which the phase diagrams have been reasonably well studied and understood. Figure 2 shows a few temperature-composition phase diagrams for lipid bilayers formed in excess water under isobaric conditions from binary lipid mixtures. It is of interest to note that the only mixture that shows complete miscibility of the chemical components in both ordered and disordered phases is one in which the two components are identical in all

respects except for a difference of two carbon atoms in their acyl chain lengths. All other systems show some degree of immiscibility either in the ordered phases and in some cases, particularly where the head groups are different, in the disordered phases as well. It is probably safe to state that in most biological membranes immiscibility in the disordered phases is more relevant since these membranes are known to be mostly fluid. The principles we shall be discussing, however, are more easily demonstrable in systems with solid-fluid phase coexistence and the lessons drawn from such models are probably equally applicable to liquid-liquid phase coexistence as well.

What causes phase coexistence in a lipid bilayer? Gibbs [17, 18] was the first to describe the conditions of chemical composition, temperature and pressure that permit phase coexistence in heterogeneous systems. Heterogeneity is a consequence of component immiscibility and the causes for this are primarily thermodynamic: the intermolecular interaction energy between two molecules in a system causes them either to associate or repel each other and entropy drives the system towards a homogenous state. This is true for any system at equilibrium. Perturbations of such systems through chemical (addition of new molecules) or physical (temperature, pressure or electrical) stresses, will cause the system to relax to a new equilibrium state at a rate that is dependent upon several processes, the kinetics of some of which may be extremely slow. It is important to remember that the biological membrane is a dynamic system, being continuously subjected to chemical and physical stresses which derive from the environment or from physiological processes such as metabolic activity of the cell and protein and lipid biogenesis, insertion and sorting [19, 20]. Hindered lateral transport [21 - 24] within the bilayer plane can make the kinetics of membrane response to these perturbations quite slow. Thus, it is very probable that the biological membrane is not a system at equilibrium and that heterogeneity in it is probably more determined by kinetic rather than by thermodynamic considerations alone.

Having accepted that heterogeneity is a fact in the biological membrane, phase disposition becomes an important consideration. Typically, in a three-dimensional fluid, phase coexistence at equilibrium is characterized by a bulk separation of the coexisting phases with a minimal interfacial area between them. The driving force for this is the interfacial surface tension which tends to reduce the interfacial area to a minimum. Reduction of the interfacial surface tension, for example by addition of surfactants to an oil-in-water or water-in-oil dispersion, reduces the tendency for bulk phase separation. In a two-dimensional system, such as the lipid bilayer, the reduction in interfacial tension is a consequence of reduced dimensionality (a two-dimensional system with an interfacial line tension as opposed to a three-dimensional system with an interfacial surface tension). Thus, one might expect microscopic to meso-

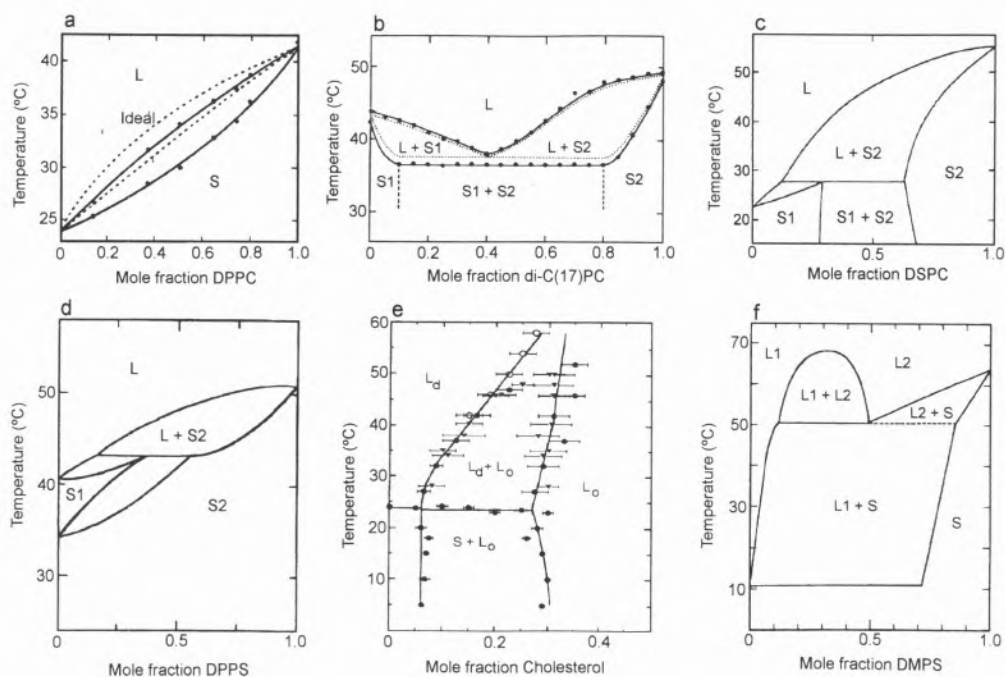


Figure 2 – Examples of temperature-composition phase diagrams for lipid bilayers in excess water under isobaric conditions. The phase diagrams are shown for: (a) isomorphous mixture of di-C(14)PC and di-C(16)PC; (b) eutectic mixture of di-C(17)PC and C(12)C(22)PC; (c) peritectic mixture of di-C(14)PC and di-C(18)PC; (d) peritectic mixture of di-C(16)PC and di-C(16)PS; (e) monotectic mixture of di-C(14)PC and cholesterol; (f) monotectic mixture of di-C(18:1, trans)PC and di-C(16)PE.

copric dispersions of coexistent phases in lipid bilayers, whether of thermodynamic or kinetic origin, to intrinsically have sufficiently long lifetimes to become physiologically relevant.

Component Distribution

From the previous section it should have become clear that we visualize the biological membrane as a heterogeneous quasi-two dimensional liquid system. The various protein species that are associated with the membrane must, strictly speaking, be viewed as chemical constituents of the system so that there is no distinction between “lipid domains” and “protein domains”. Thus, under a given compositional definition of the membrane, the protein distribution in the coexistent phases will be determined by the same rules that govern lipid distribution which have been discussed earlier. An alternative view is to consider the proteins and other minor constituents of the membrane as a very small molar fraction of the system and view them as solutes in a heterogeneous solvent. From this point of view their preferential presence in one or the other of coexistent phases in a membrane is a consequence of preferential solubility in those phases. This solubility preference can be absolute so that it becomes conceivable that a given protein species is encountered exclusively in (or totally

excluded from) one or some of several coexisting phases in the membrane.

There are several examples in the literature for solubility preferences of lipid probes and proteins in lipid bilayer membranes, the most common cases being the observed preferences of lipid-like molecules for solid or fluid phases [25 - 27]. Freeze-fracture electron microscopy studies [28] clearly show that some proteins were excluded from solid phase lipid domains in bilayers with coexisting solid and fluid phases. More recently, there has been a report [29] on the phase partitioning of gramicidin between solid and fluid phases. Fluid-fluid partitioning of lipid-like molecules and proteins has never been experimentally shown but some proteins are known to show a higher affinity for certain lipids in their boundary lipid layer [30, 31] so that it may be concluded that these proteins would necessarily show a preferential solubility in phases rich in these lipids if such phases existed in the membranes. The “hydrophobic mismatch” of an integral membrane protein in a heterogeneous fluid lipid bilayer could also be a driving force for a preferential protein solubility among the coexisting phases. We [32] have recently shown that the insertion of α -hemolysin, a protein with a membrane-inserting hydrophobic sequence, into ordered liquid phase bilayers (formed from phosphatidylcholines with a high cholesterol content) is considerably more difficult than its insertion into disordered

liquid phase bilayers (formed from pure phosphatidylcholines or binary mixtures of these with a low cholesterol content). While this in itself is not direct evidence for a preferential solubility of this protein in disordered liquid phases as compared to ordered liquid phases, it clearly indicates that such may be the case. Considerable work needs to be done in this regard before clear rules emerge for solubility preferences of lipid-like or protein molecules in lipid bilayers.

Another aspect of the heterogeneity of membrane protein distribution has to do with the way in which proteins are added to biological membranes in the process of membrane biogenesis. This process probably occurs via the intracellular fusion of vesicles with the target membrane [33]. In this case the newly inserted material must diffuse freely to become homogeneously distributed in the membrane. Hindrances to diffusion due to lack of percolation (see below) caused by intramembranous or extra-membranous (cytoskeletal or glycocalyx) structure will cause a kinetic trapping of components that may lead to physiologically significant heterogeneities.

Finally, we may imagine a protein component of a membrane which, though constrained to be integrally associated with the membrane due to its hydrophobic nature, finds no ideal solvent phase among the domains available and is forced to "precipitate" or to form homologous aggregates within the bilayer plane. Several membrane protein aggregation phenomena associated with important physiological processes are known.

Percolation

The ability of membrane components to laterally diffuse in the membrane plane is an important consequence of the fluid mosaic model for biological membrane structure and dynamics. It makes interaction between the membrane components possible, thereby permitting bi- (or higher-) molecular reactions, that are important for membrane physiology, to occur. Fluorescence Recovery After Photobleaching (FRAP) is a well established technique for the study of the lateral diffusion coefficient in two dimensional samples [24,34] (see Figure 3 for a short explanation of the method and experimental setup). This method permits observation of lateral diffusion in membranes over distances of several tens to hundreds of micrometers and is useful in studies with artificial lipid bilayers as well as with cellular membranes. In the case of synthetic bilayers the experiment is performed on a stack of a few hundred fully hydrated planar bilayers deposited on a microscope slide. These bilayers are doped with a fluorescent and photobleachable tracer molecule, which in our case is a phospholipid marked with N-(7-nitro-2,1,3-benzoxadiazol-4-yl), NBD, at a fractional molar concentration of $\leq 10^{-3}$. The general recovery behavior in homogeneous fluid bilayers is presented in Figure 4A. The

fluorescence intensity, maximum before bleaching, $F(t < 0)$, is reduced upon bleaching to $F(t = 0)$. Then, the fluorescence intensity slowly recovers due to the diffusion of neighboring tracer molecules into the bleached spot, see Figures 3a and 4. If the reservoir of unbleached molecules is infinite, as is generally the case for fluid

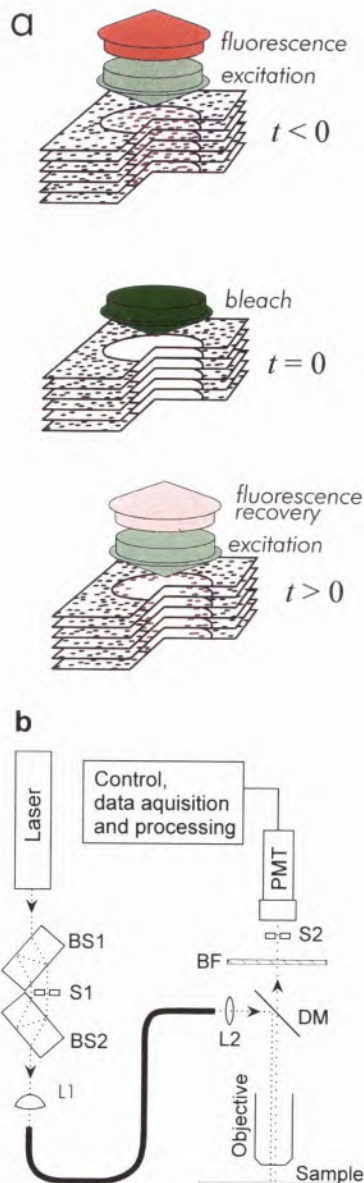


Figure 3 – Schematic description of a) a FRAP experiment performed on a stack of lipid bilayers, and b), the scheme of the FRAP apparatus where BS1 and BS2 are beam splitters, S1 the shutter that opens to bleach the sample with the intense pulse of light. Both analyzing and bleach beams are focused by L1 in an optical fiber whose output is focused by L2 through a dichroic mirror, DM, on the sample. The fluorescence is observed by a photomultiplier, PMT, protected from the intense bleaching pulse by the shutter S2, after being filtered by a cut-off filter BF.

homogeneous bilayers, the final fluorescence intensity attains the initial value $F(t=\infty)=F(t<0)$, that is, the fraction of recovery, R , defined by equation (1) is 1.0.

$$R = \frac{F(\infty) - F(0)}{F(t < 0) - F(0)} \quad (1)$$

The time dependent recovery curve, is parametrized by the translational diffusion coefficient of the tracer, D , and the radius of the circular bleaching spot, ω , according to equation (2) [35], where $\tau_D = \omega^2/4D$, and I represent Bessel functions. We may, therefore, obtain the diffusion coefficient of the tracer in the lipid matrix from the best fit between experimental data and equation (2), as shown in Figure 4.

$$F(t) = F(\infty) - [F(t < 0) - F(0)] \left\{ 1 - \exp\left(-\frac{2\tau_D}{t}\right) \left[I_0\left(\frac{2\tau_D}{t}\right) + I_1\left(\frac{2\tau_D}{t}\right) \right] \right\} \quad (2)$$

Depending on temperature, and tracer and lipid characteristics, diffusion coefficients that vary between $\approx 10^{-8}$ and $\approx 10^{-16}$ $\text{cm}^2 \text{sec}^{-1}$ have been observed. Below the ordered-disordered phase transition temperature, when the bilayer is in the so-called gel phase, the fluorescence recovery is usually very slow and incomplete over reasonable measurement times. These experimental curves, when analyzed using equation (2) often give poor fits and, if a diffusion coefficient is to be derived, values between $\approx 10^{-10}$ and as low as $[10^{-16}]$ $\text{cm}^2 \text{sec}^{-1}$ have been reported [36, 37], Figure 4B. In the rigid phase, part of the diffusion observed has been attributed to the mobility of the probe molecules in the grain boundaries of the two-dimensional crystals. In fact, the probe molecules, even if phospholipids of a very similar structure to those forming the bilayer, having the fluorescent probe attached to them, will always behave as impurities in the system with a high degree of order. In this way, some of the molecules will be retained in the crystals as point defects while other are forced into the grain boundary defects. The first group of tracer molecules is responsible for the incomplete and very slow recovery, and the second results in a recovery process that is not, in principle, described by equation (2).

In our work over the past decade we have attempted to describe the lateral diffusion of membrane components in phase-separated lipid bilayers in the phase coexistence region using the FRAP technique. While we are aware that ideally such studies, which serve as models for the biological system, should probably examine liquid-liquid phase coexistence, it is very difficult to encounter tracer molecules that partition exclusively in one of the coexisting phases with the consequence that data analysis becomes a very complex matter. For the purposes of percolation the principles governing diffusion are similar whether we examine liquid-liquid or solid-liquid phase coexistence. Our attention has, therefore, been mostly limited to bila-

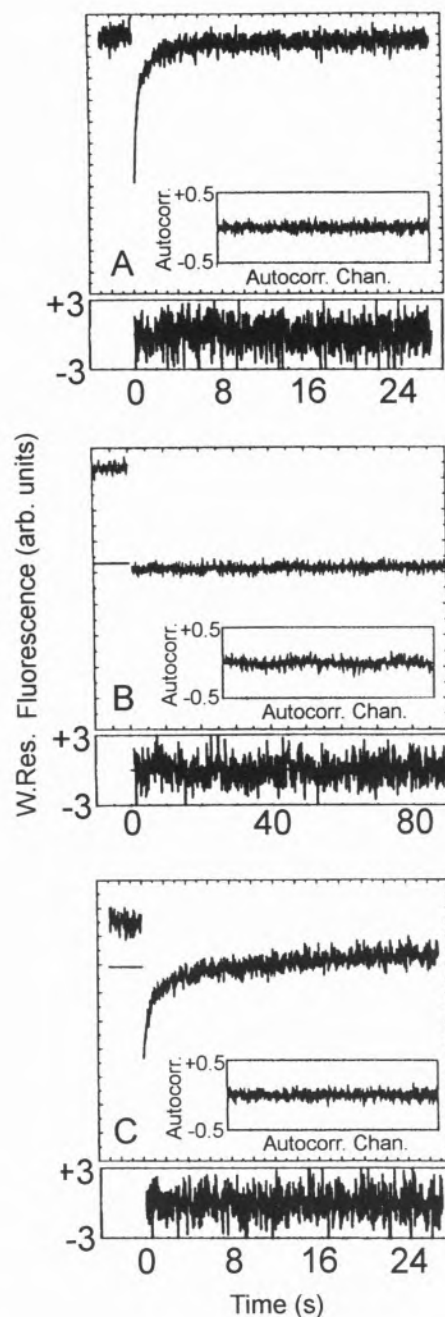


Figure 4 - Typical FRAP curves obtained for the system di- $C_{17:0}PC / C_{22:0}C_{12:0}PC$ in multibilayers. Diagram A presents the recovery of pure di- $C_{17:0}PC$ in the fluid phase, $T=52.3^\circ\text{C}$ for which 99% of recovery is observed and $\tau_D=0.21$ s (corresponding to $D=1.1 \times 10^{-7} \text{cm}^2 \text{s}^{-1}$); diagram B is for pure $C_{22:0}C_{12:0}PC$ below phase transition, $T=30.1^\circ\text{C}$, for which a τ_D ca. 200 s obtained corresponds to $D=1.1 \times 10^{-10} \text{cm}^2 \text{s}^{-1}$ and a recovery of only 3%; and diagram C is for the mixture of di- $C_{17:0}PC$ with $C_{22:0}C_{12:0}PC$ (80/20, mol/mol) in the phase coexistence region, $T=43.2^\circ\text{C}$. The analysis of the curves A and B were performed with equation (2) and for curve C an additional slope had to be used in order to obtain fit to the experimental data.

yers formed from binary lipid mixtures, in which there is a clearly defined solid-liquid phase coexistence, using probes that partition almost exclusively into the fluid phase which is the case of a short chain phospholipid in a longer chain matrix or an unsaturated phospholipid in a mixture of saturated ones. Depending on the fraction of the rigid phase, obtained from the phase diagram for the mixture, a variety of behaviors are observed [26, 38-41] as seen in Figure 4 for the system constituted by 1-docosanoyl-2-dodecanoyl-*sn*-glycero-3-phosphocholine ($C_{22:0}C_{12:0}$ PC) and 1,2-diheptadecanoyl-*sn*-glycero-3-phosphocholine ($di-C_{17:0}$ PC) [40]. For small solid fractions, the recovery of fluorescence after photobleaching is slower than what is to be expected for an equivalent fluid bilayer, but the recovery is still complete, $R \approx 1.0$. On increasing the solid fraction only a partial recovery is obtained and the recovery, fast at the beginning becomes slower for long times displaying a long tail, Figure 4C. The experimental data in this last case can no more be fitted with equation (2). It is intuitive that such behavior can be ascribed to the hindrance of diffusion by the solid domains, and to the reservoir of tracer molecules accessible to the FRAP spot being no more infinite [42].

The question arises as to what the topology of a bilayer in this phase coexisting region is, and how it relates to the experimentally observed FRAP result. It has been observed that in Langmuir-Blodgett monolayers with the same composition the phase-separation is visible with an optical fluorescence microscope and the rigid domains have a characteristic elliptical shape at the beginning, growing in spiral-like formations [43]. However, in bilayers it has not been possible to observe the domain geometry probably because, in this case, at least one of the linear dimensions of the objects is submicroscopic (smaller than the Abbé limit of $\sim \lambda/2$). Electron microscopy is not of much help because the sample preparation procedure disturbs the system, and the recent microscopic techniques with nanometer resolution, adequate for this type of samples, are yet under development. Therefore we are left with indirect methods to model the geometry of the separated phases and of the topology of the membrane. The results obtained by FRAP are, for this purpose, the most adequate because what is in fact observed is the arrival to the central spot (the photobleached area) of tracer molecules that have, on their way, sampled the intricacies of the membrane topology, i.e., we observe the result of the two-dimensional lateral molecular percolation through the system.

Percolation is a general phenomenon well known to the chemists, the percolation filter being very common in chemical industry. In the last two decades, however, a new body of theory for percolation in lattices has developed which results from the need to mathematically describe phenomena such as forest fire propagation, diffusion of small atoms in solid structures, or electrical conductivity of composite materials. All these processes fall within the area of discrete percola-

tion and are, in themselves, quite difficult to formalize mathematically. As a consequence, and given that problems in two spatial dimensions (plus time) are some of the more relevant cases of percolation, most of the practical cases are studied using straightforward Monte-Carlo techniques. Diffusion with percolation, or continuum percolation, is formally much more complicated than discrete percolation and has not yet received much attention from theoreticians. This lack of tools to deal with continuum percolation has been circumvented by the modeling of the continuum system as a discrete matrix with a lattice resolution such that the phenomena which are monitored are still described with sufficient approximation. In our study of percolation with diffusion in phase-separated synthetic bilayers we follow this approach.

The general case of diffusion in a plane in the presence of obstacles has been studied by Saxton using Monte-Carlo techniques [44]. In the diffusion in a homogeneous bilayer the mean-square displacement, $\langle r^2 \rangle$, of a molecule is proportional to the molecular diffusion coefficient, D , and to time. In obstructed diffusion the mean square displacement is still proportional to D but depends upon a fractional power of time, equation (3).

$$\langle r^2 \rangle = 4Dt (t/\tau)^{2/d_w - 1} \quad (3)$$

While for normal diffusion $d_w = 2$, in the presence of obstacles $d_w > 2$. The time constant τ is the time necessary for the probe to diffuse through the unit mean square distance. When viewed with a macroscopic technique the observed diffusion coefficient, D^* , is time dependent because the tracer molecules near the region of observation do not have to traverse the same complicated path as the more distant ones.

In a two-dimensional infinite plane of which a given fraction, p , is fluid, it has been shown that for a given geometry of the solid obstacles, randomly distributed in the plane, there is a fixed fluid fraction above which there is at least one continuous fluid cluster that connects one side of the plane with the other. This fluid fraction, characteristic of the system, is called the percolation threshold, p_c . It is important to realize that above this percolation threshold isolated finite regions of fluid do exist, but there is at least one infinite fluid cluster. Since p_c is highly dependent on the system topology we could, in principle, derive this topology from the experimental value of p_c obtained from the FRAP experiments. However, for this to be possible we first need a precise value of the percolation threshold experimentally obtained from FRAP and then need to know the shape of the elemental forms that combine to build the solid network.

To simplify the analysis of FRAP results obtained from experiments performed on systems with phase coexistence, the recovery curves were analyzed using the superposition of a fast recovery, given by equation (2), and a slow recovery, simulated by a linear ramp. The fast component describes the hindered diffusion in

an archipelago while the linear ramp models, in the experimental time range, the slow diffusion due to the defects in the gel phase. With this strategy we were able to analyze the non-conventional recovery of the fluorescence of many phospholipid systems in the region of solid-fluid phase coexistence [38-41]. In Figure 4C we present an example of the extremely good fits obtained and the data obtained from such analysis. The total recovery due only to the fast component is related to the connective fluid region that crosses the bleaching spot. At a first glance it could be suggested that since the system is either percolative or non-percolative, there should be either no recovery of fluorescence below the percolation threshold and near complete fluorescence recovery above it. However, the experimental results do not confirm these expectations as presented in Figure 5 for the system 1,2-dimyristoyl-*sn*-glycero-3-phosphocholine (DMPC) and 1,2-distearoyl-*sn*-glycero-3-phosphocholine (DSPC), 50/50 mole fraction. The sigmoid shape of the curves indicate that below p_c some flow of the tracer probe is still existent and above p_c recovery is still observed. This behavior is characteristic of percolating systems where the observation area, spot area, is of a dimension comparable with the linear dimension of the fluid regions. In figure 6 we show the theoretical variation of the fractional recovery for different relative linear dimension of the fluid areas and spot radius [45]. We may therefore conclude that whatever the geometry of the phases the dimension of the fluid phase must be of the order of magnitude of the spot radius (μm). To further define the topological characteristics of the system we have to postulate the geometric characteristics of the elements that constitute the rigid phase and verify if the resulting structure is coherent with the existing experimental data. This verification has been done by Monte-Carlo simulation of the FRAP experiments.

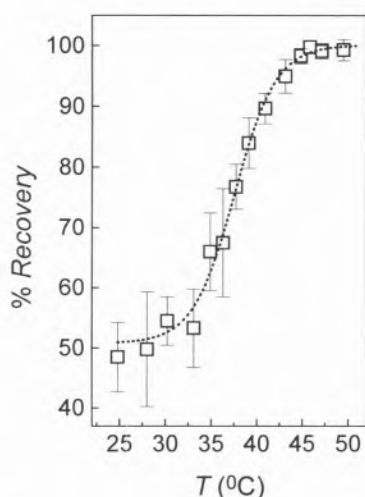


Figure 5 – Percent recovery for a DMPC / DSPC 1:1 molar fraction as a function of temperature.

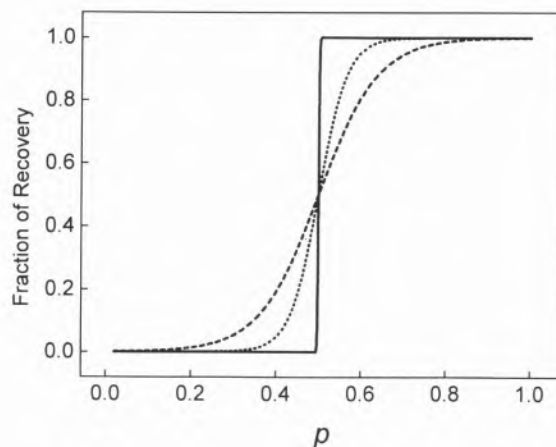


Figure 6 – Percolation theory prediction of the fraction of recovery obtained in a FRAP experiment in a system for which the percolation threshold is 0.5 for three different characteristic linear dimensions of the fluid region, L , (whatever it means in our particular case). When L is much smaller than the dimension of the spot a nearly step function is obtained, solid line, but when the observation is done with a spot similar in dimension to the characteristic dimension of the fluid there is not a well defined percolation point: dotted and dashed lines respectively for $L=20$ and 7.5 times the spot radius.

The simulation of the rigid phase as randomly distributed superimposable ellipses with aspect ratio b/a is convenient from the view point of percolation theory and reasonable with regard to two-dimensional phospholipid crystal shape. Percolation in 2D with randomly distributed ellipses has been thoroughly studied by Thorpe and coworkers [46,47] and, at least in monolayers, phospholipid crystals grow initially with a well known elliptical shape [43]. Based on this ellipse model we simulated the fractional fluorescence recovery as a function of the fluid fraction for the system DMPC: DSPC 50:50 [42]. The best fit to the high fluid fraction range was obtained for an ellipse major semi-axis of $1.0 \mu\text{m}$ and aspect ratio equal to 0.2 near the percolation threshold.

Using the same topological model, the FRAP curves simulated by Monte-Carlo in the time regime for the same system resulted in a not much different geometry of $1.0 \mu\text{m}$ and 0.3 for the major semi-axis and ellipse aspect ratio, respectively, near the percolation threshold [42]. The agreement between simulation and experiment is quite good except for fluid fractions below 0.4, Figure 7. The results from these simulations lead to a picture of the phase separated bilayer as represented in Figure 8. For large fluid fractions, Figure 8a, all the fluid is continuous but, near the percolation threshold, Figure 8b, many small regions are isolated, and for a fluid fraction of 0.2 all the fluid domains are very small, Figure 8c. In fact, the histograms of Figure 9 demonstrate that large fluid pools become highly improbable below the percolation threshold, $p_c=0.47$, and dominate immediately above it.

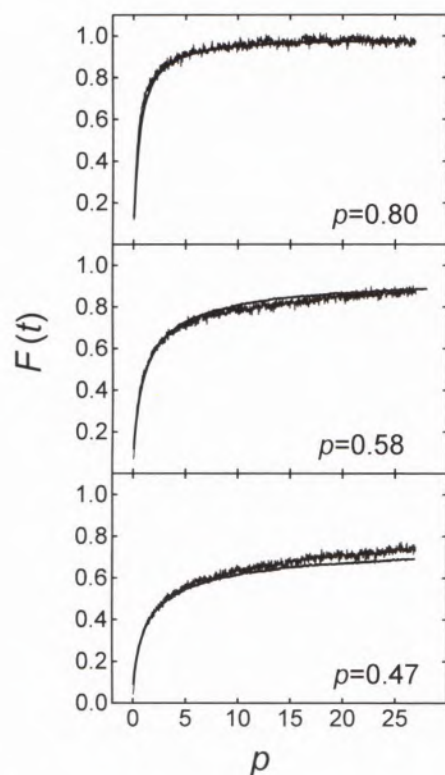


Figure 7 – Time dependent experimental fluorescence recovery curves obtained for DMPC/DSPC (1/1 mol/mol) system at three different fluid area fractions, p , and the corresponding Monte-Carlo simulations. The rigid domains were simulated as a fixed number of random ellipses that, for $p=0.80$, have semi-axes $a=0.42$ and $b=0.18$ μm ; for $p=0.58$, $a=0.88$ and $b=0.29$ μm , for $p=0.47$, $a=1.12$ and $b=0.30$ μm .

It is to be expected that molecules of reactant proteins or any other membrane components with a structure different from the lipid matrix will be more soluble in the fluid bilayer than in the more structured rigid region. Even if it is not the case those molecules that stay in the rigid phase do not have much chance to interact because of the small diffusion coefficients. In this way the compartmentalization observed results necessarily in an inhibition of bimolecular reactions taking place between membrane components.

Reactions in heterogeneous systems

When dealing with reactions in microdispersed systems two kinds of special effects have to be taken into account: dimensional, and distributional effects. The reduced dimensionality of such systems, two-dimensional, nearly-two-dimensional, or any other case where the reactants are not free to diffuse to infinite distances, do not directly affect reaction controlled processes but, in the case of diffusion controlled or nearly diffusion controlled reactions, a quite different

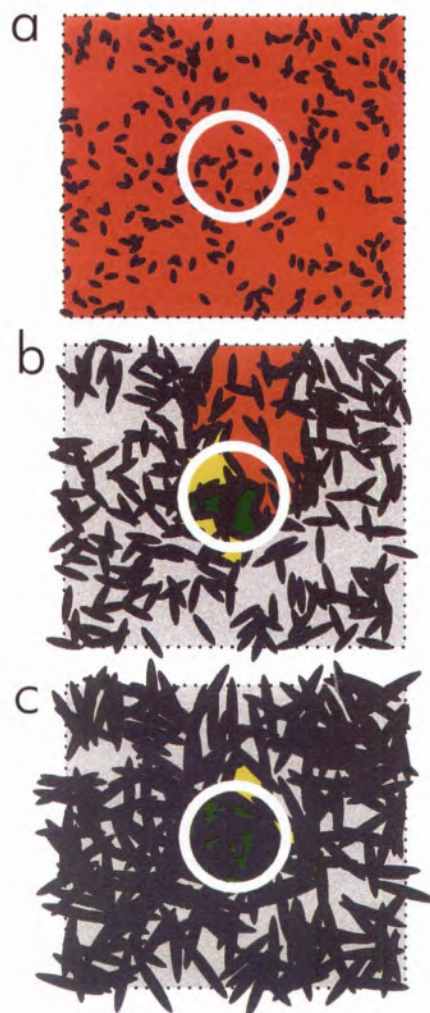


Figure 8 – Simulation of a FRAP experiment in a single bilayer plane for the DMPC/DSPC (1/1 mol/mol) system having $p_c=0.47$ for $p=0.80$ (a), 0.50 (b), and 0.20 (c). Red areas represent reservoirs that extend out of the plane (considered as completely recoverable), yellow areas partially recoverable bleached areas and those in green are unrecoverable because they are entirely closed and inside the spot.

kinetics from that expected for the equivalent 3D system is observed [48]. In what concerns the yield of the reactions, the dimensional effects will only affect those reactions for which one of the reactants is short lived. Distributional effects, however, have a marked impact upon both, the kinetics and the yield of bimolecular reactions. The consequences of distributional effects upon the yield and kinetics of reactions are better illustrated for a dimerization reaction. Consider a reaction micro-vessel where one single monomer is isolated: in this case dimerization will never take place. If, instead, two monomers are present, they dimerize, if there are three the reaction will be faster but one monomer is left unreacted. The consequences on the yield are evident,

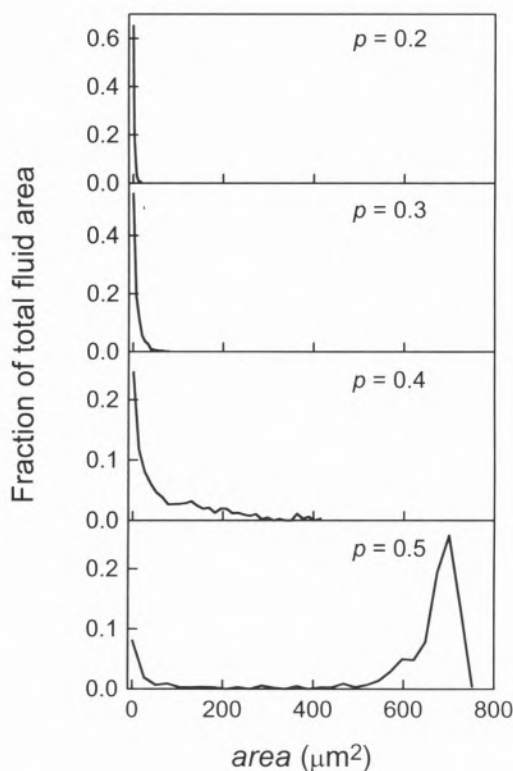


Figure 9 – Histograms of total fluid in domains with equal areas as a function of the domain areas for four different fluid fractions: $\rho=0.2, 0.3, 0.4,$ and 0.5 . It is to note that the plane, simulated as in previous figures, has a finite area of $1300 \mu\text{m}^2$ which limits the largest fluid domain present.

and it is also obvious that the global rate coefficient of dimerization will appear time dependent with some non-zero value at the beginning, and reaching zero when only isolated single molecules are left in the compartments without the possibility of reacting. From what was said we may easily anticipate that, in the case of heterobimolecular reactions where one of the reactants is in much smaller amount than the other, the difference between homogeneous and microcompartmentalized systems will be still more evident. In the extreme case of an enzymatic reaction even a small degree of compartmentalization will result in a practical inhibition of the reaction.

To quantify the extent of the inhibition of a reaction due to the membrane phase separation we define the expected relative yield as:

$$\langle \phi \rangle = \frac{\langle \Phi_{\text{ret}} \rangle}{\langle \Phi_{\text{cont}} \rangle} \quad (4)$$

where $\langle \Phi_{\text{ret}} \rangle$ is the reaction yield expected to be achieved when the membranes are reticulated (microcompartmentalized), and $\langle \Phi_{\text{cont}} \rangle$, the yield in the homoge-

neous case. However, biological systems are *a priori* compartmentalized in physically separated units such as cells, and in model lipid bilayer systems in isolated liposomes. When the conditions are such that phase separation occurs, in each of these units, U , a number N_{dom} of non-connective fluid domains is formed. If we consider that these domains are of equal size and that their number is identical in each unit, it may be shown that [49] for a reaction of an enzyme **E** with a substrate **R** catalyzing the production of product **P**, according to the reaction scheme: $\mathbf{E} + \mathbf{R} \rightarrow \mathbf{E} + \mathbf{P}$, the relative yield of **P** will be given by

$$\langle \phi \rangle = \frac{1 - \exp\left\{-\frac{[\mathbf{E}]}{[\mathbf{U}]N_{\text{dom}}}\right\}}{1 - \exp\left\{-\frac{[\mathbf{E}]}{[\mathbf{U}]}\right\}} \quad (5)$$

In Figure 10 the relative yield of product formation is represented as a function of N_{dom} for four different concentrations of the enzyme represented as $[\mathbf{E}]/[\mathbf{U}]$. It is immediately clear that the consequence of a phase separation, giving rise to non-connective fluid domains, has drastic consequences on the efficiency of the enzymatic reaction whenever the enzyme concentration is low which, in the biological system, is usually the case.

A common mechanism in cellular physiological processes is the formation of protein aggregates comprising a fixed number of monomer proteins. Also in this

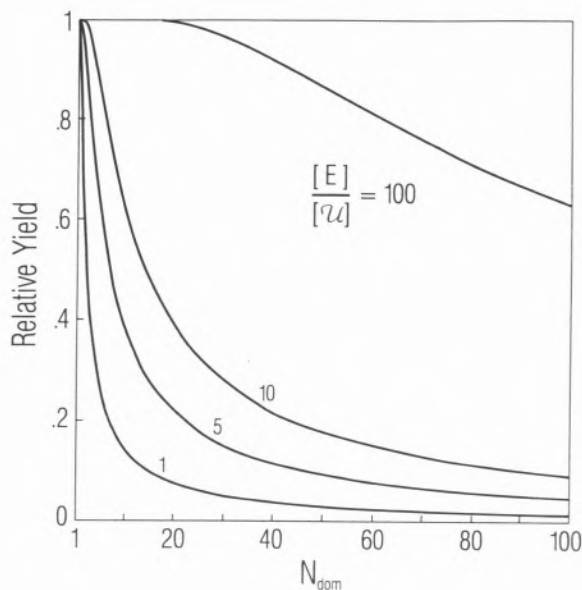


Figure 10 – Relative yield, $\langle \phi \rangle$, of product formation for a catalyzed reaction as a function of the number of domains per reaction unit, U , for different enzyme (catalyst) concentrations.

case there is a strong inhibition of the process due to isolation of the monomers in fluid non-connective domains. The relative yield for a general polymerization reaction producing aggregates of k molecules $kR \rightarrow R_k$ with $k=2, 3, \dots$ is [49]

$$\langle \phi \rangle = \frac{1 - \exp(-\mu_{ret}) \sum_{i=0}^{\infty} \sum_{j=0}^{k-1} j \frac{\mu_{ret}^{(ki+j-1)}}{(ki+j)!}}{1 - \exp(-\mu_{cont}) \sum_{i=0}^{\infty} \sum_{j=0}^{k-1} j \frac{\mu_{cont}^{(ki+j-1)}}{(ki+j)!}} \quad (6)$$

where the mean number of reactants per domain in the case of reticulated units is $\mu_{ret} = \frac{[R]}{[U]^{N_{dom}}}$ which becomes μ_{cont} for $N_{dom}=1$. For the quite common case of tetramer formation the reaction becomes inefficient even for a very small number of domains per unit, as can be seen in the representation of $\langle \phi \rangle$ as a function of N_{dom} , equation (6), for the cases of $k=2, 3$ and 4 , Figure 11.

It is clear that in the real case of a phospholipid mixture below the percolation threshold, all these physiologically relevant reactions will become highly improbable and by changing the physical-chemical state of their membrane a cell could, in principle, control many of its metabolic steps.

The effect on the yields is accompanied by a no less noticeable modification of the reaction kinetics. We have studied the kinetics of photodimerization of 12-(9-anthroxyloxy) stearic acid, 12AS, in a model system cons-

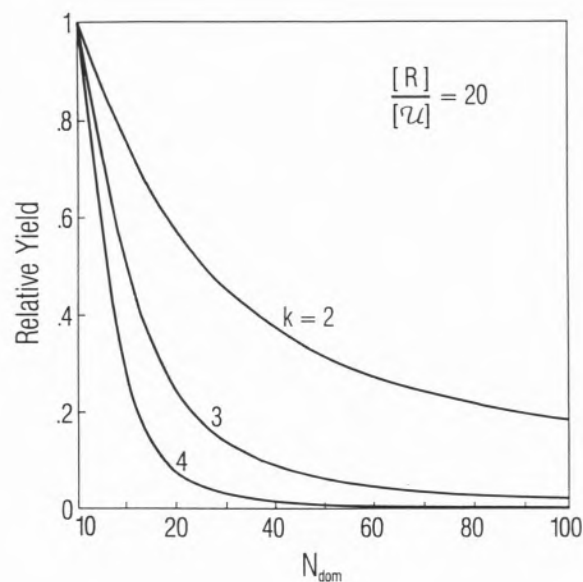
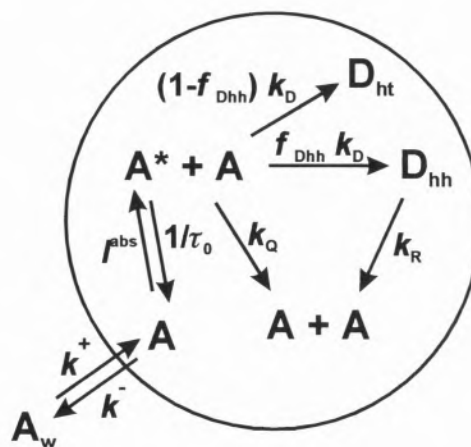


Figure 11 – Relative yield of a polymerization reaction for 20 monomers per unit as a function of the number of domains per unit. Plots are presented for the case of dimer ($k=2$), trimer ($k=3$), and tetramer ($k=4$).

tituted by a dispersion of cetyltrimethylammonium chloride, CTAC, and polyoxyethylene(10) lauryl ether, $C_{12}E_{10}$, micelles [50]. In these systems two different dimers are formed, one thermally unstable head-to-head dimer, D_{hh} , and a stable head-to-tail dimer, D_{ht} . The global kinetic scheme of the reaction in micelles, including the steps of exit and entrance of the monomer, A, in the micelles, is presented in the Scheme I. The exit steps are slow, as can be seen in Table I where the relevant rate constants involved in the process are presented, but for large irradiation times they lead to the randomization of the system [50]. The relative order of magnitude of the rate constants involved, is similar to what is to be expected for phospholipid bilayers with non-connective fluid domains: the reaction is nearly diffusion controlled, and the interchange of molecules between micelles model quite well the possible leakage of reagents between separated fluid domains observed in bilayers.



Scheme I

Table I - Steady-state photodimerization rate constant, k_D , association rate constant, k^+ , and exit rate constant, k^- , for 12-(9-anthroxyloxy) stearic acid, 12AS, in micelles of cetyltrimethylammonium chloride, CTAC, and polyoxyethylene(10) lauryl ether, $C_{12}E_{10}$, according to Scheme I.

Surfactant	k_D ($10^7 M^1 s^{-1}$)	k^+ ($10^{10} M^{-1} s^{-1}$)	k^- ($10^{-3} s^{-1}$)
CTAC	2.2	1.2	0.7
$C_{12}E_{10}$	8.9	1.6	30.

In Figure 12 a simulation of our system in CTAC, irradiated with a typical light intensity and in the absence of water solubility of the reagents, displaying the time dependence of the apparent rate coefficient for the reaction defined as

$$k_{app} = \frac{d[A_2]}{dt [A][A^*]} \quad (7)$$

is presented for several occupation numbers. The value of the time-independent rate constant for a homogeneous phase with the same characteristics of the micelle media is also shown for comparison. Due to the large number of molecules left unreacted when the occupation number is small, see insert of Figure 12 where the yield of the reaction is presented, the apparent rate coefficient attains values near zero immediately after the beginning of the irradiation.

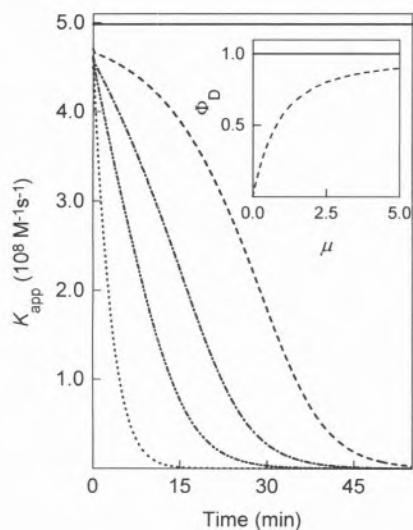


Figure 12 – Theoretical simulation of a non-reversible photodimerization reaction in a micellar system without exchange of monomers between micelles. Variation of $k_{app} = (d[A_2]/dt)/[A][A^*]$, with time of irradiation for mean occupation values of 0.3 (---), 1.0 (---), 2.0 (---), and 5.0 (---). The solid horizontal line, at the top, indicates the rate constant of the same reaction in a homogeneous media with identical characteristics. Inset: efficiency of dimerization in the homogeneous (—) and compartmentalized (---) system as a function of the mean occupation number, μ .

The effect of the rate of entrance and exit from the micelles, k^+ and k^- , is to reduce the difference between homogeneous and compartmentalized media but, as may be seen in Figure 13, only when the interchange is quite fast the behavior approaches the one observed for homogeneous media. It should, however, be noted that, once interchange is considered, the theoretical relative yield of the reaction is unity no matter how much time the system will need to approach this maximum yield [50].

The results obtained with this micellar system show how important the distribution of reactants in non-communicating compartments can be for the kinetics of a bimolecular reaction triggered by an external factor, light in our case.

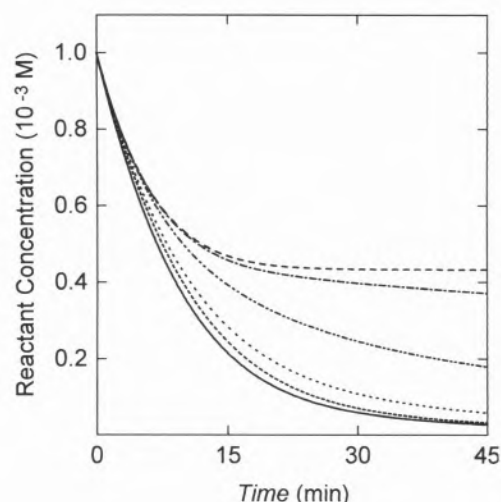


Figure 13 – Theoretical simulation of the disappearance of reactant concentration as a function of time in a photodimerization reaction in micelles when exchange between micelles is considered and compared with the reaction in homogeneous phase (—). Curves are plot for $k^- (s^{-1}) = 0.0$ (---), 1×10^{-4} (---), 1×10^{-3} (---), 1×10^{-2} (---), 1×10^{-1} (---), 10.0 (---).

Relevance to Biological Systems

In a recent paper we have discussed several consequences of phase separations in membranes [9]. What follows will be a brief synopsis of those considerations.

Biological membranes are the interface of communication between the cell and its environment. Reception and processing of information from the environment will, therefore, be conditioned by the ability of the membrane to respond to external stimuli so that the consequences of heterogeneity in this structure could be quite significant. Processing of information involves membrane protein activity at the unimolecular (first order reaction) level and the ability of membrane components to react with each other at the multimolecular (second or higher order reactions) level.

Conformation and dynamics of proteins, and as a consequence their activity, is largely conditioned by the environment. When a membrane protein encounters itself in a given membrane phase, the physical (fluidity and lateral pressure) and chemical (ionic environment, charge and hydrogen-bonding ability) properties of that phase may condition the activity of the protein [31]. This concept can be applied to membrane-bound enzymes and receptors. The relationship between membrane lipid environment and membrane enzyme activity has been well studied and it is not uncommon in receptor biochemistry and pharmacology to encounter multiple affinities of a single receptor species in a membrane for its ligand.

Without excluding other plausible explanations, we propose that these multiple affinities may be a consequence of multiplicity of membrane environments for the receptor population in a given membrane as the consequence of phase coexistence in it.

As shown in the preceding sections, the effects of membrane heterogeneity on reaction yields and reaction kinetics can be quite significant. When reactants are micro-compartmentalized, reaction yields are, in the extreme case, limited to encounters at the phase boundaries which implies a slow reaction rate and very low reaction yields. In homogenous media the reactions proceed to completion at a considerably faster, often diffusion-controlled, rate. As a consequence, transitions between heterogeneous and homogenous states, induced by physical and/or chemical processes, will imply simultaneous transitions in the rate and yields of chemical reactions that occur in the system and could act as trigger processes that may be important in cell physiology.

Assuming that membrane components (proteins and lipids) show preferential partitioning (solubility) behavior in different coexistent membrane phases, the existence of heterogeneity raises questions with regard to long-range diffusivity of these components. The range and rate of diffusion is, as discussed earlier, a function of the percolative properties of the membrane lipid bilayer. A considerable body of evidence indicates that protein diffusion in cellular plasma membranes is generally hindered. This has been generally attributed to various types of associative interactions of these proteins both within and outside the membrane but can also be interpreted in terms of the percolative behavior in a heterogeneous membrane context [9].

Finally, microscopic and mesoscopic domains in a membrane may be diffusionally trapped by specific binding interactions of one or more of their components with structures that are external to the cell. Situations can be visualized in which such a diffusional trapping forces domains of an identical phase to come in contact with each other so that the phase boundary between them disappears and the domain size grows. This sort of growth can eventually lead to a macroscopic phase separation as is seen in many cells. Elsewhere [9] we have hypothetically described the formation of apical and basolateral domains and the formation of the tight junction in epithelia.

Bibliography

1. E. Gorter, F. Grendel (1925) *J. Exper. Med.* **41**, 439-443.
2. J.F. Danielli, H. Davson (1935) *J. Cell. Comp. Physiol.* **5**, 595-610.
3. J.D. Robertson (1959) *Biochem. Soc. Symp.* **16**, 3-43.
4. S.J. Singer, G.L. Nicolson (1972) *Science* **175**, 720-731.
5. S.H. Wu, H.M. McConnell (1975) *Biochemistry* **14**, 847-854.
6. D. Marsh (1990) CRC Handbook of Lipid Bilayers, pp. 234-263, CRC Press, Boca Raton, FL.
7. K. Simons, S.D. Fuller (1985) *Ann. Rev. Cell Biol.* **1**, 243-288.

8. W.H. Evans (1980) *Biochim. Biophys. Acta* **604**, 27-64.
9. W.L.C. Vaz (1996) In: Handbook of Non-Medical Applications of Liposomes, Vol. II: Models of Biological Phenomena (Y. Barenholz, D. Lasic, editors), Ch. 3, pp. 51-60, CRC Press, Boca Raton, FL.
10. K. Huang (1987) In: Statistical Mechanics, 2nd. edition, pp. 408-412, John Wiley, New York.
11. M.K. Jain (1983) In: Membrane Fluidity in Biology (R.C. Aloia, editor), pp. 1-37, Academic Press, New York.
12. W.L.C. Vaz, P.F.F. Almeida (1993) *Current Opin. Struct. Biol.* **3**, 482-488.
13. K. Jacobson, W.L.C. Vaz, editors (1992) Comments on Molecular and Cellular Biophysics Vol. 8: Domains in Biological Membranes, Gordon & Breach, London.
14. W.L.C. Vaz (1994) *Biophys. Chem.* **50**, 139-145.
15. G. Ceve, D. Marsh (1987) Phospholipid Bilayers: Physical Principles and Models, John Wiley, New York.
16. H. Träuble (1977) In: 34th. Nobel Symposium: Structure of Biological Membranes (S. Abrahamsson, I. Pascher, editors), pp. 509-550, Plenum Press, New York.
17. J.W. Gibbs (1877) *Trans. Connecticut Acad.* **3**, 108-248.
18. J.W. Gibbs (1877) *Trans. Connecticut Acad.* **3**, 343-524.
19. M.P. Lisanti, E. Rodriguez-Boulan (1990) *Trends Biochem. Sci.* **15**, 113-118.
20. K. Simons, G. van Meer (1988) *Biochemistry* **27**, 6197-6202.
21. R.M. Clegg, W.L.C. Vaz (1985) In: Progress in Protein-Lipid Interactions, Vol 1 (A. Watts, J.J.H.M. De Pont, editors), pp. 73-229, Elsevier, Amsterdam.
22. W.L.C. Vaz, F. Goodsaid-Zalduondo, K. Jacobson (1984) *FEBS Letters* **174**, 199-207.
23. K. Jacobson, A. Ishihara, R. Inman (1987) *Ann. Rev. Physiol.* **49**, 163-175.
24. T.M. Jovin, W.L.C. Vaz (1989) In: Methods in Enzymology, Vol. 172, (S. Fleischer, B. Fleischer, editors), pp. 471-513, Academic Press, New York.
25. L.A. Sklar, G.P. Miljjanich, E.A. Dratz (1979) *Biochemistry* **18**, 1707-1716.
26. W.L.C. Vaz, E.C.C. Melo, T.E. Thompson (1989) *Biophys. J.* **56**, 869-876.
27. J.F. Tocanne (1992) *Comments Mol. Cell. Biophys.* **8**, 53-72.
28. W. Kleemann, H.M. McConnell (1974) *Biochim. Biophys. Acta* **345**, 220-230.
29. A.R.G. Dibble, M.D. Yeager, G.W. Feigenson (1993) *Biochim. Biophys. Acta* **1153**, 155-162.
30. D. Marsh (1987) *J. Bioenerg. Biomemb.* **19**, 677-689.
31. P.F. Devaux, M. Seigneuret (1985) *Biochim. Biophys. Acta* **822**, 63-125.
32. I. Bakás, H. Ostolaza, W.L.C. Vaz, F.M. Goñi (1996) *Biophys. J.* **71**, 1869-1876.
33. I. Mellman, editor (1996) *Current Opinion Cell Biol.* **8**(4), 497-574
34. W.L.C. Vaz, Z.I. Derzko, K. Jacobson (1982) In: Cell Surface Reviews, Vol. 8: Membrane Reconstitution (G. Poste, G.L. Nicolson, editors), pp. 83-136, Elsevier, Amsterdam.
35. D.M. Soumpasis (1983) *Biophys. J.* **41**, 95-97
36. Z. Derzko, K. Jacobson (1980) *Biochemistry* **19**, 6050-6057.
37. M.B. Schneider, W.K. Chan, W.W. Webb (1983) *Biophys. J.* **43**, 157-165.
38. W.L.C. Vaz, E.C.C. Melo, T.E. Thompson (1990) *Biophys. J.* **58**, 273-275.
39. T. Bultmann, W.L.C. Vaz, E.C.C. Melo, R.B. Sisk, T.E. Thompson (1991) *Biochemistry* **30**, 5573-5579.
40. P.F.F. Almeida, W.L.C. Vaz, T.E. Thompson (1992) *Biochemistry* **31**, 7198-7210.
41. P.F.F. Almeida, W.L.C. Vaz, T.E. Thompson (1993) *Biophys. J.* **64**, 399-412.
42. F.P. Coelho, W.L.C. Vaz, E. Melo (1997) *Biophys. J.* **72**, 1501-1511.
43. D.J. Keller, J.P. Korb, H.M. McConnell (1987) *J. Phys. Chem.* **91**, 6417-6422.
44. M.J. Saxton (1994) *Biophys. J.* **66**, 394-401
45. P.F.F. Almeida (1992) Ph.D. Dissertation, University of Virginia.
46. W. Xia, M.F. Thorpe (1988) *Phys. Rev. A* **38**, 2650-2656.
47. E.J. Garboczi, M.F. Thorpe, M.S. De Vries, A.R. Day (1991) *Phys. Rev. A* **43**, 6473-6482.
48. J. Martins, W.L.C. Vaz, E. Melo (1996) *J. Phys. Chem.* **100**, 1889-1895
49. E.C.C. Melo, I.M.G. Lourtie, M.B. Sankaram, T.E. Thompson, W.L.C. Vaz (1992) *Biophys. J.* **63**, 1506-1512.
50. M.J. Moreno, I.M.G. Lourtie, E. Melo (1996) *J. Phys. Chem.* **100**, 18192-18200.

